

# Transformation of Sc<sub>2</sub>O<sub>3</sub>-doped tetragonal zirconia polycrystals by aging under hydrothermal conditions

M. HIRANO, E. KATO

Department of Applied Chemistry, Aichi Institute of Technology, Yachigusa, Yakusa, Toyota, 470-0392 Japan  
E-mail: hirano@ac.aitech.ac.jp

The phase transformation of less than 6 mol % Sc<sub>2</sub>O<sub>3</sub>-doped tetragonal zirconia polycrystals consisting of fine grains has been investigated. Dense bodies with homogeneous microstructures doped with 3.5 to 5 mol % Sc<sub>2</sub>O<sub>3</sub> sintered at 1300 °C for 1 h consisted mostly of a tetragonal phase. Within 20 h of aging under hydrothermal conditions at 180 °C, the amount of monoclinic ZrO<sub>2</sub> on the surface of the 4 to 5 mol % Sc<sub>2</sub>O<sub>3</sub>-doped specimens sintered at 1400 °C was saturated and reached a constant value, and the increase in the amount of monoclinic ZrO<sub>2</sub> showed a sigmoidal type of kinetic transformation. The apparent activation energy for the phase transformation in Sc<sub>2</sub>O<sub>3</sub>-doped zirconia was 84–91 kJ/mol. Based on the hydrothermal aging results, the possible existence of a larger two-phase (cubic+tetragonal) region is suggested, and the phase boundary between the cubic+tetragonal and cubic phase in the ZrO<sub>2</sub>-Sc<sub>2</sub>O<sub>3</sub> system is proposed. © 1999 Kluwer Academic Publishers

## 1. Introduction

The properties of zirconia-based materials significantly depend on the stabilizing agent and its concentration. Sc<sub>2</sub>O<sub>3</sub>-doped zirconia at close to 8 mol % Sc<sub>2</sub>O<sub>3</sub> content has been shown to possess a higher oxygen ion mobility than Y<sub>2</sub>O<sub>3</sub>-doped zirconia at elevated temperature [1, 2]. Sc<sub>2</sub>O<sub>3</sub>-doped zirconia is more suitable for the practical application as a solid electrolyte used in the construction of high-temperature fuel cells. Studies of the ZrO<sub>2</sub>-Sc<sub>2</sub>O<sub>3</sub> phase diagram and fabrication, and electrical and mechanical properties of Sc<sub>2</sub>O<sub>3</sub>-doped zirconia have been published [1–21]. On the other hand, the addition of Y<sub>2</sub>O<sub>3</sub> to ZrO<sub>2</sub> over a wide range of concentration for stabilization as the tetragonal and cubic forms as well as for fabrication techniques which consists of the tetragonal phase were also investigated by a number of researchers [22–25], in the ZrO<sub>2</sub>-Y<sub>2</sub>O<sub>3</sub> system. In particular, Y<sub>2</sub>O<sub>3</sub>-doped tetragonal zirconia polycrystals, prepared by fine particle technology, exhibit high strength and high toughness at room temperature and they are currently being used as structural ceramics. In the Y<sub>2</sub>O<sub>3</sub>-doped tetragonal zirconia, one problem is that their mechanical properties and microstructure were significantly decreased by low temperature aging at 200 to 300 °C in air, which is caused by the tetragonal-to-monoclinic phase transformation on the surface accompanied by microcracking [26–29]. Many studies on the low temperature degradation and on degradation inhibition have also been carried out [30–46].

In the ZrO<sub>2</sub>-Sc<sub>2</sub>O<sub>3</sub> system, a degradation in conductivity for 9 mol % Sc<sub>2</sub>O<sub>3</sub>-doped zirconia after aging at an elevated temperature of 800 to 1000 °C for any length of time was reported and this behavior was attributed to the formation of an ordered rhombohedral  $\beta$ -phase (Sc<sub>2</sub>Zr<sub>7</sub>O<sub>17</sub>) [47]. A similar aging behavior for the degradation of the microstructure and conductivity of 7 to 8 mol % Sc<sub>2</sub>O<sub>3</sub>-doped zirconia was also investigated by researchers [16, 48]. Yamamoto *et al.* [49] have examined the phase change of 8 mol % Sc<sub>2</sub>O<sub>3</sub>-doped zirconia using a Raman scattering technique and concluded that the conductivity decrease of 8 mol % Sc<sub>2</sub>O<sub>3</sub>-doped zirconia by annealing at 1000 °C for 5000 h is attributed to the phase change from cubic to tetragonal. On the other hand, Badwal and Drennan [17] have shown that 8 mol % Sc<sub>2</sub>O<sub>3</sub>-doped zirconia is not cubic and has a tetragonal symmetry with small tetragonal splitting, and the  $\beta$ -phase is not observed in any of the specimens fabricated by sintering of the coprecipitated powders. Ishii *et al.* [15] reported that the crystal structure of 12 mol % Sc<sub>2</sub>O<sub>3</sub>-doped zirconia changed from rhombohedral to cubic at the transition temperature with a discontinuous change in the ion conductivity. It has been reported that the cubic phase with fast ion conductivity is stabilized in the low temperature region by substitution of a dopant such as 2 mol % Gd<sub>2</sub>O<sub>3</sub>-10 mol % Sc<sub>2</sub>O<sub>3</sub> [15] for 12 mol % Sc<sub>2</sub>O<sub>3</sub>-doped zirconia and by the dispersion of 0.3–20 mass % Al<sub>2</sub>O<sub>3</sub> [14, 19] in 11–12 mol % Sc<sub>2</sub>O<sub>3</sub>-doped zirconia. However, in the ZrO<sub>2</sub>-Sc<sub>2</sub>O<sub>3</sub> system, sufficient information on the properties of the Sc<sub>2</sub>O<sub>3</sub>-doped zirconia

containing less than 7 mol %  $\text{Sc}_2\text{O}_3$  is still lacking. There are few reports on the tetragonal-to-monoclinic phase transformation of the dense  $\text{Sc}_2\text{O}_3$ -doped tetragonal zirconia polycrystals by low temperature aging except for arc-melted samples [50].

In the present study, dense  $\text{Sc}_2\text{O}_3$ -doped tetragonal zirconia polycrystals with a fine grain were prepared using fine powders synthesized by hydrolysis and homogeneous precipitation. Special attention was paid to their low temperature aging behavior and tetragonal-to-monoclinic phase transformation.

## 2. Experimental procedure

### 2.1. Samples

In the present study, 3 to 7 mol %  $\text{Sc}_2\text{O}_3$ -doped fine zirconia powders were used for sintering, which were prepared by the urea-based homogeneous precipitation method using the monoclinic zirconia sol previously formed by the hydrolysis of  $\text{ZrOCl}_2$  solution. Aqueous solutions of zirconium oxychloride ( $\text{ZrOCl}_2 \cdot 8\text{H}_2\text{O}$ ) (0.1 mol/l) were hydrolyzed by heating at  $100^\circ\text{C}$  for 170 h to produce a sol containing ultrafine monoclinic zirconia particles [51]. The sol solution was added to an aqueous solution in which a given quantity of scandia was dissolved by nitric acid, then added to urea solution and kept at  $90^\circ\text{C}$  with stirring. The resultant homogeneous precipitates were separated, washed, dried, calcined at  $600^\circ\text{C}$  in air, and then milled with zirconia balls in ethanol. Thus, fine zirconia powders were prepared as the starting materials. The powders were cold-pressed at 98 MPa to form pellets. The green compacts were sintered at 1300 to  $1600^\circ\text{C}$  for 1 h in air.

### 2.2. Aging and measurements

To evaluate the resistance of the tetragonal to monoclinic phase transformation, the sintered samples and distilled water was treated at a saturated water pressure from 110 to  $180^\circ\text{C}$  for 2 to 55 h using 25 ml Teflon vessels housed in an outer pressure vessel made of stainless steel. They were placed in a drying oven controlled with a thermostat in order to heat the samples at the desired temperature. The sealed vessels were quickly cooled to room temperature. The bulk density of the sintered bodies were measured using Archimedes technique. Phase identification was carried out by X-ray diffraction analysis of the flat surface of the specimen. Scans of  $2\theta$  between  $27^\circ$  and  $33^\circ$  were conducted to quantify the monoclinic zirconia volume fraction using the following equation: monoclinic (%) =  $\frac{\{\text{monoclinic (111)} + \text{monoclinic (11}\bar{1})\}}{\{\text{tetragonal and cubic (111)} + \text{monoclinic (111)} + \text{monoclinic (11}\bar{1})\}} \times 100$ . The microstructure of the surface of the thermal etched samples and cut surface of the aged samples were analyzed by AFM and SEM.

## 3. Results and discussion

### 3.1. Characteristics of as-sintered materials

The relationship between the  $\text{Sc}_2\text{O}_3$  content and relative density of the  $\text{Sc}_2\text{O}_3$ -doped zirconia sintered bodies

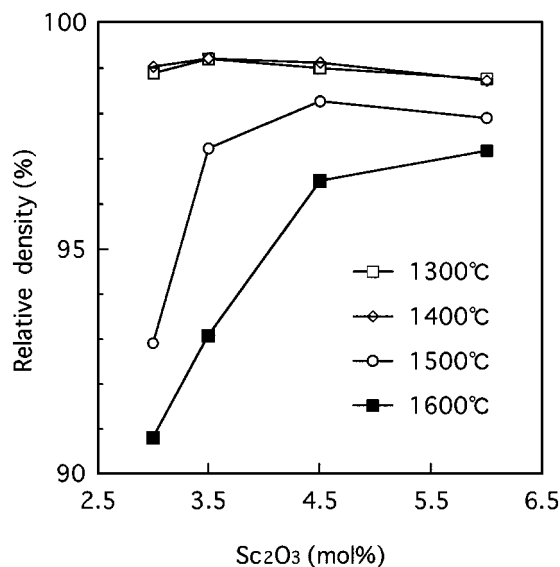


Figure 1 Relationship between  $\text{Sc}_2\text{O}_3$  content and relative density of the  $\text{Sc}_2\text{O}_3$ -doped zirconia ceramics sintered at 1300 to  $1600^\circ\text{C}$  for 1 h.

fabricated at 1300 to  $1600^\circ\text{C}$  is shown in Fig. 1. For calculating the relative density, the theoretical density of the  $\text{Sc}_2\text{O}_3$ -doped zirconia was determined using the unit cell volume data [7]. Relative density reached almost 99% of theoretical at a sintering temperature of 1300 or  $1400^\circ\text{C}$ , but it decreased with increasing sintering temperature in all samples. In the samples containing less than 3.5 mol %  $\text{Sc}_2\text{O}_3$ , it showed a remarkable decrease in relative density at sintering temperatures of 1500 and  $1600^\circ\text{C}$ .

The relation between  $\text{Sc}_2\text{O}_3$  content and the amount of monoclinic  $\text{ZrO}_2$  in the as-sintered bodies is shown in Fig. 2. Although the amount of monoclinic  $\text{ZrO}_2$  in the sintered bodies increased with increasing sintering temperature, it was found that no monoclinic

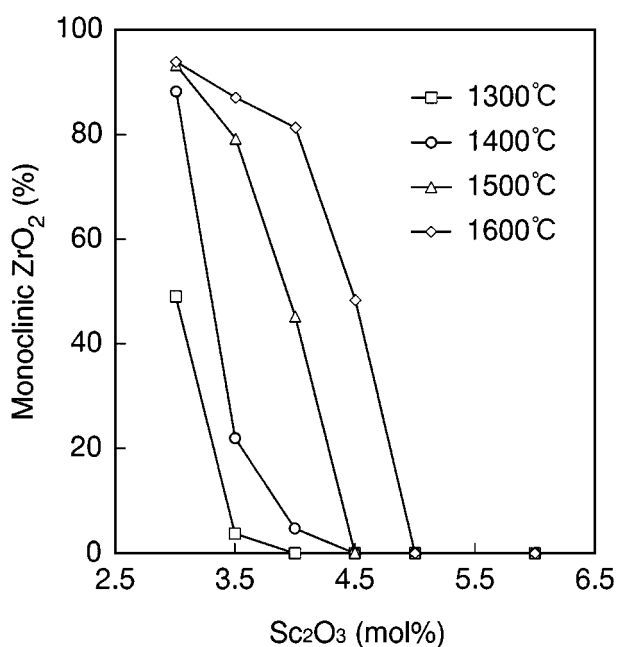


Figure 2 Change in the amount of monoclinic zirconia phase with  $\text{Sc}_2\text{O}_3$  content on the surface of the  $\text{Sc}_2\text{O}_3$ -doped zirconia ceramics sintered at 1300 to  $1600^\circ\text{C}$  for 1 h.

ZrO<sub>2</sub> was detected in the as-sintered bodies containing 5 and 6 mol % Sc<sub>2</sub>O<sub>3</sub>-doped zirconia fabricated at 1300 to 1600 °C for 1 h. At a sintering temperature of 1300 °C, dense sintered bodies mostly consisting of the tetragonal phase were obtained in the range of 3.5 to 5 mol % Sc<sub>2</sub>O<sub>3</sub>. The decrease in relative density in the samples containing less than 4 mol % Sc<sub>2</sub>O<sub>3</sub> sintered at 1500 and 1600 °C may be due to the discrepancy between the calculated theoretical density based on a tetragonal structure, the true density of the sintered body containing a high amount of monoclinic phase and the microcracking caused by the tetragonal-to-monoclinic phase transformation.

The typical microstructure of 4 mol % Sc<sub>2</sub>O<sub>3</sub>-doped zirconia sintered at 1400 °C is shown in Fig. 3. The microstructure of the as-sintered specimens consisted of small grains of uniform grain size. The average grain size and its distribution of materials with different Sc<sub>2</sub>O<sub>3</sub> contents are shown in Fig. 4.

The grain growths of the 4 and 5 mol % Sc<sub>2</sub>O<sub>3</sub>-doped zirconia fabricated at 1400 to 1600 °C are shown in Fig. 5. The average grain size of the 4 mol % Sc<sub>2</sub>O<sub>3</sub>-doped zirconia sintered at 1400 °C was <0.5 μm. It may be considered that the gradual decrease in the relative density of the specimens containing above 4.5 mol % Sc<sub>2</sub>O<sub>3</sub> sintered at 1500 and 1600 °C is mainly responsible for the rapid grain growth that is produced during the heating process from 1400 to 1600 °C and for the change in the ratio of the tetragonal and cubic phase content. The microstructure was similar to that of zirconia ceramics in the ZrO<sub>2</sub>-Y<sub>2</sub>O<sub>3</sub> system but the addition of a larger amount of stabilization agent (nearly 1.5 times, i.e., 3.5 mol % Sc<sub>2</sub>O<sub>3</sub> at sintering temperature of 1400 °C) was necessary for fabricating the sintered bodies consisting of a fully tetragonal phase in the ZrO<sub>2</sub>-Sc<sub>2</sub>O<sub>3</sub> system. The average grain size, its distribution, and crystal phase of the ZrO<sub>2</sub> (+Sc<sub>2</sub>O<sub>3</sub>) materials were found to significantly depend on the Sc<sub>2</sub>O<sub>3</sub> content and sintering temperature.

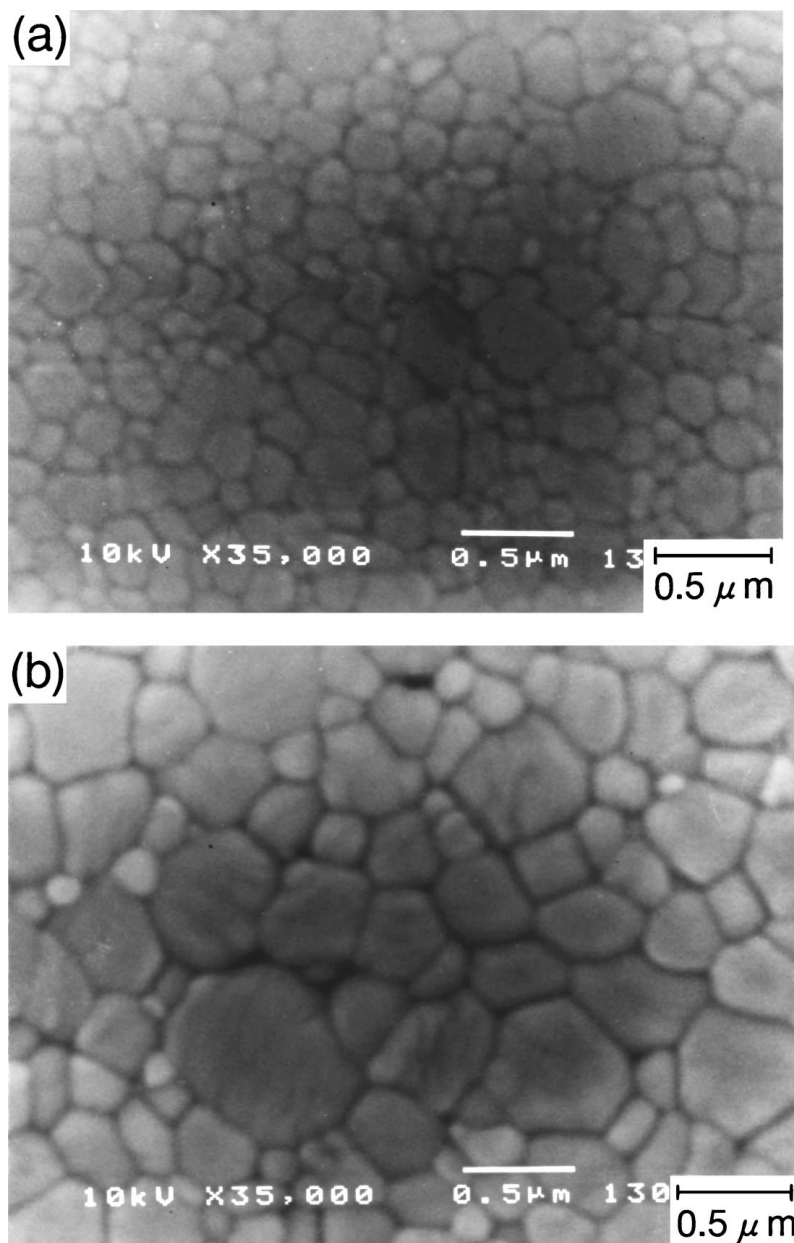


Figure 3 SEM photographs of the polished and thermally etched surface of the 4 mol % Sc<sub>2</sub>O<sub>3</sub>-doped zirconia ceramics sintered at (a) 1300 °C and (b) 1400 °C for 1 h.

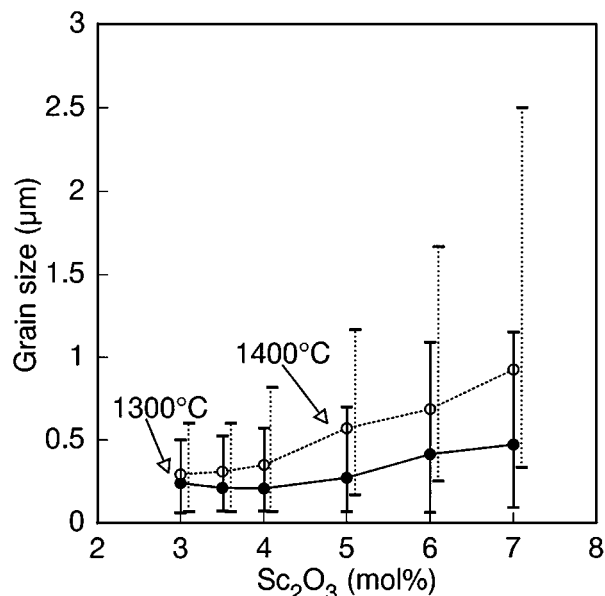


Figure 4 Relationship between grain size and its distribution and  $\text{Sc}_2\text{O}_3$  content of the  $\text{Sc}_2\text{O}_3$ -doped zirconia ceramics.

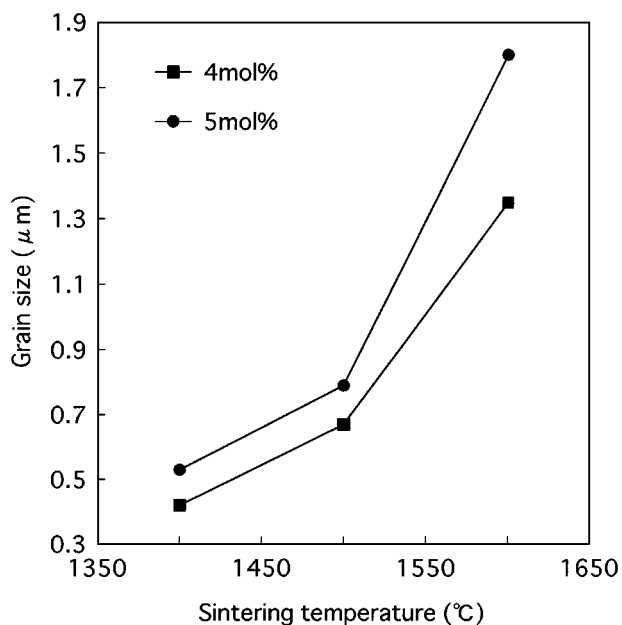


Figure 5 Relationship between grain size and sintering temperature for the 4 mol% and 5 mol%  $\text{Sc}_2\text{O}_3$  doped zirconia ceramics.

### 3.2. Tetragonal-to-monoclinic phase transformation of $\text{Sc}_2\text{O}_3$ -doped zirconia

The monoclinic  $\text{ZrO}_2$  content formed on the surface of the tetragonal zirconia ceramics, containing 4 to 6 mol%  $\text{Sc}_2\text{O}_3$  fabricated at  $1400^\circ\text{C}$ , by aging under hydrothermal conditions at  $180^\circ\text{C}$  is shown in Fig. 6 as a function of aging time. As indicated in Figs 4 and 5, the average grain sizes of the samples are in the submicron range and they have a relatively uniform microstructure and dense body as given in Fig. 1. On the surface of these as-sintered materials, no monoclinic phase was detected by X-ray diffraction analysis except for the 4 mol%  $\text{Sc}_2\text{O}_3$ -doped zirconia with a small amount of monoclinic  $\text{ZrO}_2$  ( $\leq 3\%$ ). The amount of monoclinic  $\text{ZrO}_2$  reached nearly a saturated and constant value within 20 h in the 4 to 5 mol%  $\text{Sc}_2\text{O}_3$ -doped specimens. On the other hand,

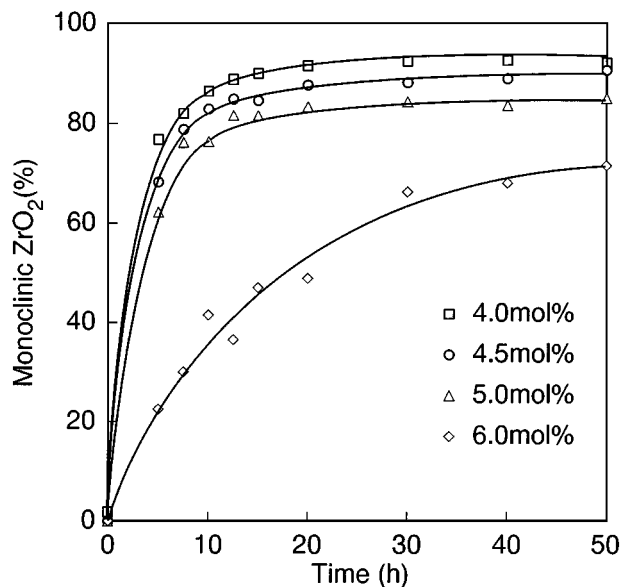


Figure 6 Tetragonal-to-monoclinic phase transformation resulting from hydrothermal aging at  $180^\circ\text{C}$  for the  $\text{Sc}_2\text{O}_3$ -doped zirconia ceramics sintered at  $1400^\circ\text{C}$  for 1 h.

in the 6 mol%  $\text{Sc}_2\text{O}_3$ -doped zirconia, the amount of monoclinic  $\text{ZrO}_2$  slowly increased after the same 20 h aging time. The final amounts of monoclinic  $\text{ZrO}_2$  for the 4, 4.5, 5, and 6 mol%  $\text{Sc}_2\text{O}_3$ -doped specimens were 93, 91, 85, and 72%, respectively. In the  $\text{ZrO}_2$ - $\text{Y}_2\text{O}_3$  system, the 5 mol%  $\text{Y}_2\text{O}_3$ - $\text{ZrO}_2$  ceramics did not indicate a monoclinic formation and a phase transformation after aging at  $200^\circ\text{C}$  in air [52], but a single cubic phase with a grain size of  $2.3 \mu\text{m}$  was obtained in the 6.6 mol%  $\text{Y}_2\text{O}_3$ - $\text{ZrO}_2$  sintered at  $1400^\circ\text{C}$  for 1 h [53]. Nakajima *et al.* [54] reported that the saturated monoclinic fraction of 2.5, 3.5, 4.5, and 5 mol%  $\text{Y}_2\text{O}_3$ -doped zirconia, which were sintered at  $1550^\circ\text{C}$  for 2 h, aged under hydrothermal conditions at  $180^\circ\text{C}$  were 90, 70, 40, and 30%, respectively.

In Fig. 7, the relationship between the  $\text{R}_2\text{O}_3$  content and the saturated volume fraction of the monoclinic phase in  $\text{ZrO}_2$ - $\text{R}_2\text{O}_3$  samples hydrothermally treated is shown on the basis of the data in Fig. 6. This figure also includes the data that was determined

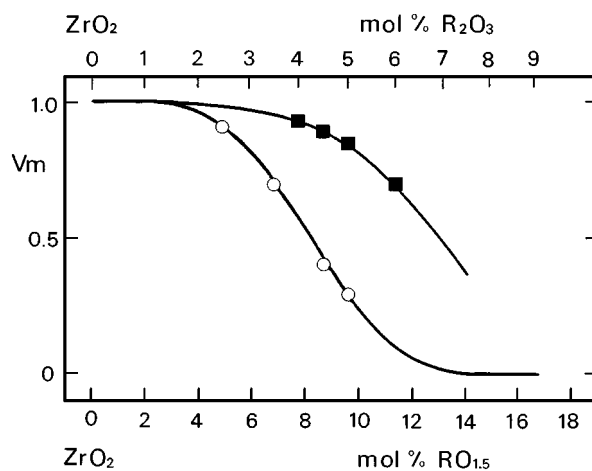


Figure 7 Relationship between  $\text{R}_2\text{O}_3$  content and volume fraction of saturated monoclinic phase in the  $\text{ZrO}_2$ - $\text{R}_2\text{O}_3$  sintered bodies:  $\text{ZrO}_2$ - $\text{Y}_2\text{O}_3$  system (samples sintered at  $1550^\circ\text{C}$ ):  $\circ$  [54];  $\text{ZrO}_2$ - $\text{Sc}_2\text{O}_3$  system (samples sintered at  $1400^\circ\text{C}$ ):  $\blacksquare$  [present work].

using polycrystalline samples sintered at 1550 °C in the ZrO<sub>2</sub>-Y<sub>2</sub>O<sub>3</sub> system reported by Nakajima *et al.* [54]. Because the tetragonal fractions are changeable based on the cooling process, the actual tetragonal fractions of the as-sintered specimens are somewhat different from those obtained in an equilibrium state at the sintering temperature. However, these saturated values of volume fraction of monoclinic ZrO<sub>2</sub> should be considered to correspond to the metastable tetragonal phase content that existed at room temperature and also the stable tetragonal phase content that existed at the sintering temperature. In the ZrO<sub>2</sub>-Y<sub>2</sub>O<sub>3</sub> system, the ratio of the metastable tetragonal phase (=volume fraction of monoclinic phase in Fig. 7) and cubic phase (=untransformed phase) was in good agreement with the value in equilibrium at 1550 °C in the presented phase diagrams [55–57]. Whereas in the ZrO<sub>2</sub>-Sc<sub>2</sub>O<sub>3</sub> system, the ratio of the tetragonal and cubic phases in the polycrystalline sample sintered at 1400 °C and the phase boundary between the cubic+tetragonal and cubic phases do not correspond to the presented phase diagram [10]. There is the possible existence of a larger two-phase (tetragonal+cubic) region than those in the phase diagram. Yamamoto *et al.* [49] also recently reported that the as-sintered 8 mol % Sc<sub>2</sub>O<sub>3</sub>-doped zirconia polycrystalline sample fabricated at 1700 °C for 15 h showed a mixture of tetragonal and cubic phases by a Raman scattering study, which also does not correspond to the phase diagram [10]. Although the purpose in this study is not the presentation of the phase diagram, based on the results in this study and the report [49], the phase boundary between the cubic+tetragonal and cubic phases has been proposed as indicated in Fig. 8.

The time dependences of monoclinic ZrO<sub>2</sub> formation for the 4.5 and 6 mol % Sc<sub>2</sub>O<sub>3</sub>-doped zirconia sintered at 1400 °C are shown in Figs. 9a and b, and they also indicate the effect of aging temperature on the phase transformation. A sigmoidal type of kinetics transformation on aging of the Sc<sub>2</sub>O<sub>3</sub>-doped tetragonal zirconia is evident from these illustrations and this

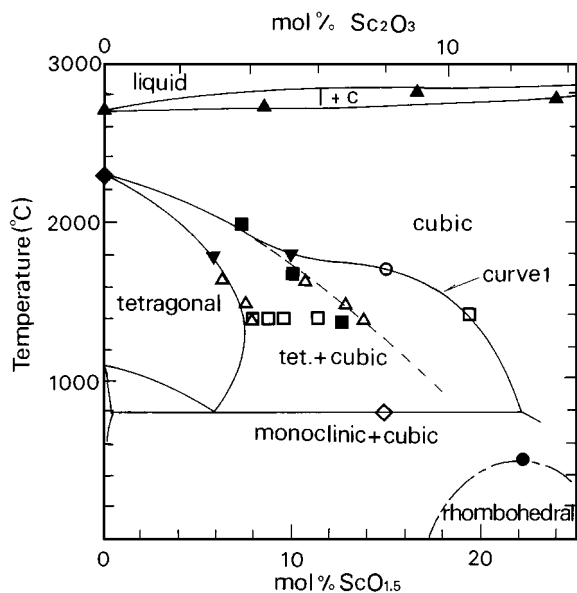


Figure 8 Phase diagram in the ZrO<sub>2</sub>-Sc<sub>2</sub>O<sub>3</sub> system, ▲ [2]; ■ [1]; △ [5]; ▼ [6]; ◇ [7]; ● [8]; ◆ [9]; ○ [49]; □ [present work]; curve 1 [proposed phase boundary based on the present study].

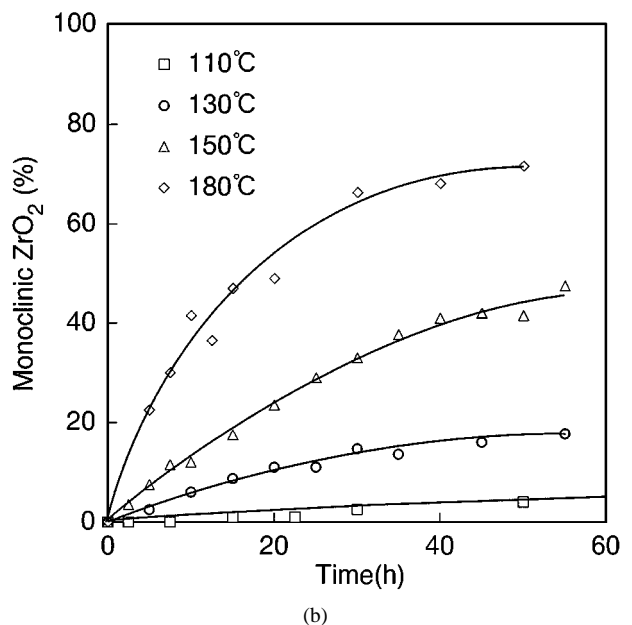
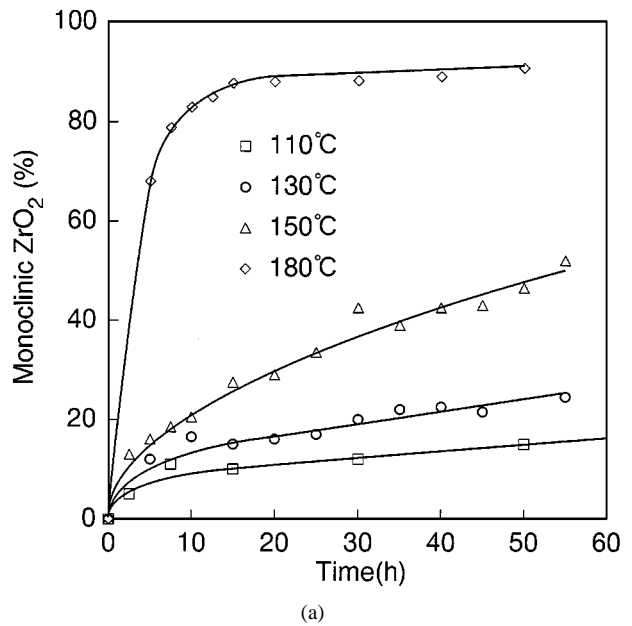


Figure 9 Relationship between the amount of the monoclinic phase and aging time under hydrothermal conditions at 110 to 180 °C for the (a) 4.5 mol % and (b) 6 mol % Sc<sub>2</sub>O<sub>3</sub>-doped zirconia ceramics sintered at 1400 °C for 1 h.

behavior is similar to the case of the Y<sub>2</sub>O<sub>3</sub>-doped or CeO<sub>2</sub>-doped tetragonal zirconia [34, 54, 58]. Though hydrothermal aging was conducted only up to 180 °C in this experiment, the phase transformation rate increased with increasing aging temperature.

Based on the results in Figs. 9a and b, first-order kinetics plots of  $\ln\{1/(1 - \alpha)\}$  vs. time for the monoclinic ZrO<sub>2</sub> formation on the surface of the 4.5 and 6 mol % Sc<sub>2</sub>O<sub>3</sub>-doped zirconia are shown in Figs. 10a and b, respectively, where  $\alpha$  is the fractional conversion of the tetragonal ZrO<sub>2</sub> to monoclinic ZrO<sub>2</sub>. For the other samples, the measured values were also plotted in a similar manner. Note that these data were corrected by taking into account the amount of tetragonal ZrO<sub>2</sub>, which was converted to monoclinic ZrO<sub>2</sub>, being 93, 91, 85, and 72 % in the 4, 4.5, 5, and 6 mol % Sc<sub>2</sub>O<sub>3</sub>-doped zirconia specimens, respectively. The plots of  $\ln\{1/(1 - \alpha)\}$  vs. time were linear. The rate of phase transformation on

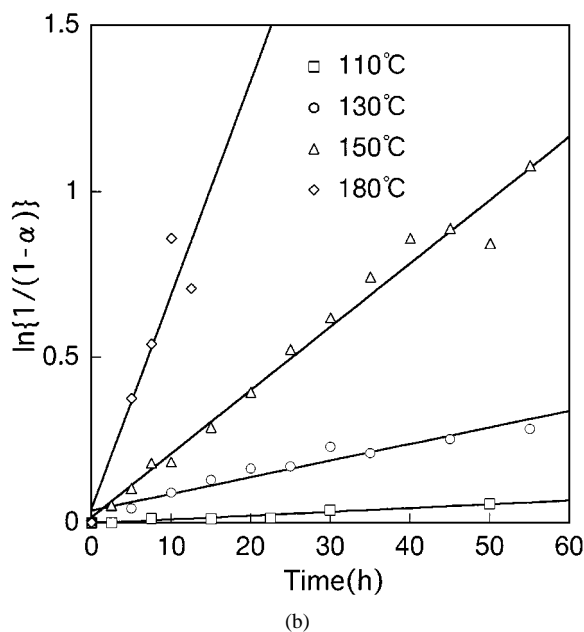
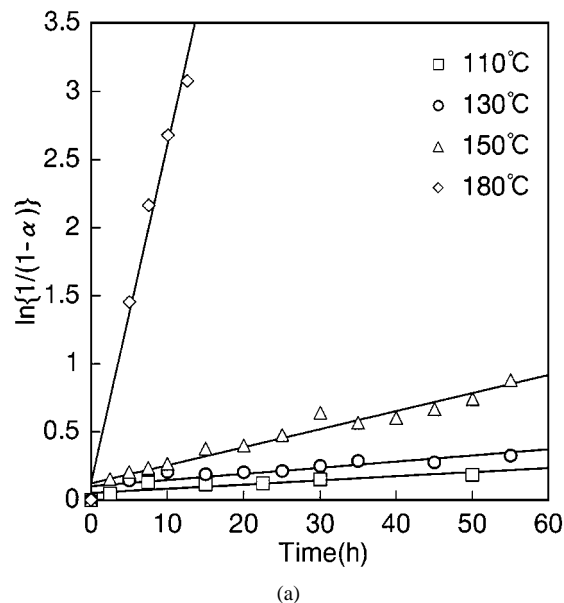


Figure 10 Plots of  $\ln\{1/(1-\alpha)\}$  vs. time for the tetragonal-to-monoclinic phase transformation in the (a) 4.5 mol % and (b) 6 mol %  $\text{Sc}_2\text{O}_3$ -doped zirconia ceramics.

the surface was first order with regard to the tetragonal phase concentration.

In Fig. 11, the Arrhenius plots of the rate constant of the tetragonal-to-monoclinic phase transformation in zirconia ceramics doped with 4, 4.5, 5, and 6 mol %  $\text{Sc}_2\text{O}_3$  are indicated. The apparent activation energies were 91.4, 89.1, 90.4, and 84.3 kJ/mol for the 4, 4.5, 5, and 6 mol %  $\text{Sc}_2\text{O}_3$ -doped zirconia specimens, respectively, which were very similar to the value of 83.1–92.4 kJ/mol [28, 58] obtained for the  $\text{Y}_2\text{O}_3$ -doped or  $\text{CeO}_2$ -doped tetragonal zirconia.

A transformed layer was clearly observed in each specimen aged under hydrothermal conditions at 180 °C for greater than 10 h. The monoclinic phase was formed on the surface of the specimen and the transformation progressed and invaded the inside of the body accompanied by microcracking with time. In the  $\text{ZrO}_2$ - $\text{Y}_2\text{O}_3$  system, Lange *et al.* [29] reported that the degradation of the  $\text{Y}_2\text{O}_3$ -doped tetragonal zirconia

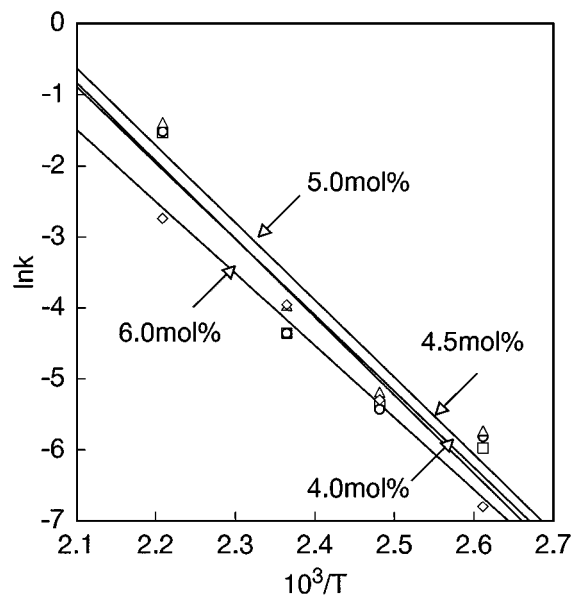


Figure 11 Arrhenius plots of the rate constant of the tetragonal-to-monoclinic phase transformation in the 4.0 to 6.0 mol %  $\text{Sc}_2\text{O}_3$ -doped zirconia ceramics.

during aging at 250 °C was caused by the reaction of water with  $\text{Y}_2\text{O}_3$  in the tetragonal zirconia solid solution to produce monoclinic nuclei that spontaneously grew, provoking the transformation of tetragonal grains and subsequent crack formation. Sato and Shimada [28] reported that the phase transformation rate was controlled by the chemical reaction between water absorbed on the surface and the Zr-O-Zr band. Yoshimura *et al.* [59] attributed the degradation of the  $\text{Y}_2\text{O}_3$ -doped tetragonal zirconia under hydrothermal conditions to a diffusion process controlled by  $\text{OH}^-$  migration.

Although there are many explanations for this phase transformation and degradation behavior, many researchers agreed with the theory of a critical grain size below which degradation could be avoided. In the study of the low temperature degradation of seven  $\text{Y}_2\text{O}_3$ -doped tetragonal zirconia materials, one specimen with a fine-grained microstructure (mean grain size = 0.18  $\mu\text{m}$ ) showed no physical or property degradation after exposure to a water vapor pressure for 50 h between 200 and 400 °C [60]. It was also reported that  $\text{Y}_2\text{O}_3$ -doped tetragonal zirconia with an extremely low grain size (=0.1  $\mu\text{m}$ ) can suppress the chemical degradation of the material [61]. In  $\text{Sc}_2\text{O}_3$ -doped tetragonal zirconia, it is considered that the stability of the tetragonal phase can be enhanced in the same manner as in the case of  $\text{Y}_2\text{O}_3$ -doped tetragonal zirconia, so a fine-grained microstructure is necessary and grain size control is important if a  $\text{Sc}_2\text{O}_3$ -doped tetragonal zirconia is to resist low temperature degradation.

#### 4. Summary

The low temperature aging behavior and tetragonal-to-monoclinic phase transformation of  $\text{Sc}_2\text{O}_3$ -doped tetragonal zirconia polycrystals with a submicron microstructure (3–6 mol %  $\text{Sc}_2\text{O}_3$  content) under hydrothermal conditions have been investigated. The amount of monoclinic  $\text{ZrO}_2$  nearly reached saturation and a constant value within 20 h in the 4 to 5 mol %  $\text{Sc}_2\text{O}_3$  doped specimens and it showed a sigmoidal

type of kinetic transformation. The rate of phase transformation on the surface was first order with regard to the tetragonal phase concentration. The apparent activation energies were 84 to 91 kJ/mol for the 4 to 6 mol% Sc<sub>2</sub>O<sub>3</sub>-doped zirconia specimens, respectively, which were almost similar to the value obtained for the Y<sub>2</sub>O<sub>3</sub> doped or CeO<sub>2</sub>-doped tetragonal zirconia. We have suggested the possible existence of a larger two-phase (cubic+tetragonal) region based on the hydrothermal aging results.

## References

1. F. M. SPIRIDONOV, L. N. POPOVA and YA. POPILSKII, *J. Solid State Chem.* **2** (1970) 430.
2. R. RUH, H. J. GARRETT, R. F. DOMAGALA and V. A. PATEL, *J. Amer. Ceram. Soc.* **60** (1977) 399.
3. M. R. THORNER, D. J. M. BEVAN and E. SUMMERVILLE, *J. Solid State Chem.* **1** (1970) 545.
4. R. L. MAGUNOV, G. L. SHKLYAR and V. F. KATRIDI, *Inorg. Mater.* **25** (1989) 1035.
5. T. S. SHEU, J. XU and T.-Y. TIEN, *J. Amer. Ceram. Soc.* **76** (1993) 2027.
6. M. J. BANNISTER and P. F. SKILTON, *J. Mater. Sci. Lett.* **2** (1983) 561.
7. T. S. SHEU, T. Y. TIEN and I. W. CHEN, *J. Amer. Ceram. Soc.* **75** (1992) 1108.
8. J. LEFEVRE, *Ann. Chim.* **8** (1963) 117.
9. P. ALDEBERT and J.-P. TRAVERSE, *J. Amer. Ceram. Soc.* **68** (1985) 34.
10. M. YASHIMA, N. ISHIZAWA, H. FUJIMORI, M. KAKIHANA and M. YOSHIMURA, *Eur. J. Solid State and Inorg. Chem.* **32** (1995) 761.
11. M. YASHIMA, M. KAKIHANA and M. YOSHIMURA, *Solid State Ionics* **86-88** (1996) 1131.
12. D. W. STRICKER and W. G. CARLSON, *J. Amer. Ceram. Soc.* **48** (1965) 286.
13. O. YAMAMOTO, T. KAWAHARA, Y. TAKEDA, N. IMANISHI and Y. SAKAKI, "Science and Technology of Zirconia V" (Technomic, USA, 1993) p. 733.
14. O. YAMAMOTO, Y. ARATI, Y. TAKEDA, N. IMANISHI, Y. MIZUTANI, M. KAWAI and Y. NAKAMURA, *Solid State Ionics* **79** (1995) 137.
15. T. ISHII, T. IWATA and Y. TAJIMA, *ibid.* **57** (1992) 153.
16. F. K. MOGHADAM, T. YAMASHITA, R. SINCLAIR and D. A. STEVENSON, *J. Amer. Ceram. Soc.* **66** (1983) 213.
17. S. P. S. BADWAL and J. DRENNAN, *Solid State Ionics* **53-56** (1992) 769.
18. F. TIETX, W. FISCHER, TH. HAUBER and G. MARIOTTO, *ibid.* **100** (1997) 289.
19. Y. MIZUTANI, M. TAMURA, M. KAWAI and O. YAMAMOTO, *ibid.* **72** (1994) 271.
20. M. HIRANO and E. KATO, *J. Ceram. Soc. Japan* **105** (1997) 37.
21. M. HIRANO, S. WATANABE, E. KATO, Y. MIZUTANI, M. KAWAI and Y. NAKAMURA, *Solid State Ionics* **111** (1998) 161.
22. T. K. GUPTA, J. H. BECHTOLD, R. C. KUZNICKI, L. H. CADOFF and B. R. ROSSING, *J. Mater. Sci.* **12** (1977) 2421.
23. F. F. LANGE, *ibid.* **17** (1982) 240.
24. T. K. GUPTA, F. F. LANGE and J. H. BECHTOLD, *ibid.* **13** (1978) 1464.
25. I. NETTLESHIP and R. STEVENS, *Int. J. High Technol. Ceram.* **3** (1987) 1.
26. K. KOBAYASHI, H. KUWAJIMA and T. MASAKI, *Solid State Ionics* **3/4** (1981) 489.
27. T. SATO and M. SHIMADA, *J. Amer. Ceram. Soc.* **67** (1984) c-212.
28. *Idem.*, *ibid.* **68** (1985) 356.
29. F. F. LANGE, G. L. DUNLOP and B. I. DAVIS, *ibid.* **69** (1986) 237.
30. M. HIRANO, *Brit. Ceram. Trans. J.* **91** (1992) 139.
31. E. LILLEY, in "Ceramic Transactions," Vol. 10, edited by R. E. Tressler and M. McNallen (The American Ceramic Society, Westerville, OH, 1990) p. 387.
32. T. T. LEPISTO and T. A. MANTYLA, in "Corrosion of Glass, Ceramics and Ceramic Superconductors; Principles, Testing, Characterization and Applications," edited by D. E. Clark and B. K. Zaitos (Noyes, Park Ridge, NJ, 1992) p. 492.
33. M. MATSUI, T. SOMA and I. ODA, "Advances in Ceramics," Vol. 12 (The American Ceramic Society, Westerville, OH, 1984) p. 371.
34. H.-Y. LU and S.-Y. CHEN, *J. Amer. Ceram. Soc.* **70** (1987) 537.
35. M. KAGAWA, M. OMORI, Y. SYONO, Y. IMAMURA and S. USUI, *ibid.* **70** (1987) c-212.
36. N. NARITA, S. LENG, T. INADA and K. HIGASHIDA, in "Sintering 87, Proceedings of the International Institute for the Science of Sintering Symposium, Tokyo, Japan, 1987," edited by S. Somiya, M. Shimada, M. Yoshimura and R. Watanabe (Elsevier Applied Science, London, NY, Tokyo, 1988) p. 1130.
37. S. IIO, M. WATANABE, K. KURODA, H. SAKA and T. IMURA, "Advances in Ceramics," Vol. 24 (The American Ceramic Society, Westerville, OH, 1989) p. 49.
38. N. NAKANISHI and T. SHIGEMATSU, *Mater. Trans. JIM.* **32** (1991) 778.
39. H. TSUBAKINO, R. NOZATO and M. HAMAMOTO, *J. Amer. Ceram. Soc.* **74** (1991) 440.
40. W. Z. ZHU, T. C. LEI and Y. ZHOU, *J. Mater. Sci.* **28** (1993) 6479.
41. C. B. AZZONI, A. PALEARI, F. SCARDINA, A. KRAJEWSKI, A. RAVAGLIOLI and F. MESCHKE, *ibid.* **28** (1993) 3951.
42. G. BEHRENS, G. W. DRANSMANN and A. H. HEUER *J. Amer. Ceram. Soc.* **76** (1993) 1025.
43. Y. SAKKA, *J. Mater. Sci. Lett.* **11** (1992) 18.
44. A. E. HUGHES, F. T. CIACCHI and S. P. S. BADWAL, in "Science and Technology of Zirconia V," edited by S. P. S. Badwal, M. J. Bannister and R. H. J. Hannink (Technomic, Lancaster, PA, 1993) p. 152.
45. O. KRUSE, H. D. CARSTANJEN, P. W. KOUNTOUROS, H. SCHUBERT and G. PETZOW, in "Science and Technology of Zirconia V," edited by S. P. S. Badwal, M. J. Bannister and R. H. J. Hannink (Technomic, Lancaster, PA, 1993) p. 163.
46. J.-K. LEE and H. KIM, *J. Mater. Sci.* **29** (1994) 136.
47. M. V. INOZEMTSEV, M. V. PERFILEV and V. P. GORELOV, *Sov. Electrochem.* **12** (1976) 1128.
48. F. K. MOGHADAM, PhD thesis, Stanford University, 1981.
49. O. YAMAMOTO, Y. ARACHI, K. NOMURA, Y. MIZUTANI, M. KAWAI and Y. NAKAMURA, Extended Abstract Electrochem. Soc., Fall Meeting, San Antonio, Vol. 96-2, 1996, p. 763.
50. M. YASHIMA, T. NAGATOME, T. NOMA, N. ISHIZAWA, Y. SUZUKI and M. YOSHIMURA, *J. Amer. Ceram. Soc.* **78** (1995) 2229.
51. Y. MURASE, E. KATO and M. HIRANO, *Yogyo Kyokaishi (J. Ceram. Soc. Japan)* **92** (1984) 64.
52. T. MASAKI, *Int. J. High. Technol. Ceram.* **2** (1986) 85.
53. F. F. LANGE, *J. Amer. Ceram. Soc.* **69** (1986) 240.
54. K. NAKAJIMA, K. KOBAYASHI and Y. MURATA, in "Advances in Ceramics," Vol. 12, edited by N. Claussen, M. Ruhle and A. H. Heuer (American Ceramic Society, Columbus, OH, 1984) p. 399.
55. H. G. SCOTT, *J. Mater. Sci.* **10** (1975) 1527.
56. R. RUH, K. S. MAZDIYASNI, P. G. VALENTINE and H. O. BIELSTEIN, *J. Amer. Ceram. Soc.* **67** (1984) C190.
57. M. YOSHIMURA, *Amer. Ceram. Soc. Bull.* **67** (1988) 1950.
58. T. SATO and M. SHIMADA, *ibid.* **64** (1985) 1382.
59. M. YOSHIMURA, T. NOMA, K. KAWABATA and S. SOMIYA, *J. Mater. Sci. Lett.* **6** (1987) 465.
60. J. J. SWAB, *J. Mater. Sci.* **26** (1991) 6706.
61. A. J. A. WINNUBST and A. J. BURGRAAF, in "Advances in Ceramics," Vol. 24, edited by S. Somiya, N. Yamamoto and H. Yanagida (American Ceramic Society, Westerville, OH, 1988) p. 39.

Received 7 February  
and accepted 4 November 1998